Archival Report

Biological Psychiatry: CNNI

Inhaled Cannabis Suppresses Chemotherapy-Induced Neuropathic Nociception by Decoupling the Raphe Nucleus: A Functional Imaging Study in Rats

Ilayda Alkislar, Alison R. Miller, Andrea G. Hohmann, Aymen H. Sadaka, Xuezhu Cai, Praveen Kulkarni, and Craig F. Ferris

ABSTRACT

BACKGROUND: Efficacy of inhaled cannabis for treating pain is controversial. Effective treatment for chemotherapy-induced neuropathy represents an unmet medical need. We hypothesized that cannabis reduces neuropathic pain by reducing functional coupling in the raphe nuclei.

METHODS: We assessed the impact of inhalation of vaporized cannabis plant (containing 10.3% Δ^9-tetrahydrocannabinol/0.05% cannabidiol) or placebo cannabis on brain resting-state blood oxygen level–dependent functional connectivity and pain behavior induced by paclitaxel in rats. Rats received paclitaxel to produce chemotherapy-induced peripheral neuropathy or its vehicle. Behavioral and imaging experiments were performed after neuropathy was established and stable. Images were registered to, and analyzed using, a 3D magnetic resonance imaging rat atlas providing site-specific data on more than 168 different brain areas.

RESULTS: Prior to vaporization, paclitaxel produced cold allodynia. Inhaled vaporized cannabis increased cold withdrawal latencies relative to prevaporization or placebo cannabis, consistent with Δ^9-tetrahydrocannabinol-induced antinociception. In paclitaxel-treated rats, the midbrain serotonergic system, comprising the dorsal and median raphe, showed hyperconnectivity to cortical, brainstem, and hippocampal areas, consistent with nociceptive processing. Inhalation of vaporized cannabis uncoupled paclitaxel-induced hyperconnectivity patterns. No such changes in connectivity or cold responsiveness were observed following placebo cannabis vaporization.

CONCLUSIONS: Inhaled vaporized cannabis plant uncoupled brain resting-state connectivity in the raphe nuclei, normalizing paclitaxel-induced hyperconnectivity to levels observed in vehicle-treated rats. Inhaled vaporized cannabis produced antinociception in both paclitaxel- and vehicle-treated rats. Our study elucidates neural circuitry implicated in the therapeutic effects of Δ^9-tetrahydrocannabinol and supports a role for functional imaging studies in animals in guiding indications for future clinical trials.

https://doi.org/10.1016/j.bpsc.2020.11.015

Chemotherapy-induced peripheral neuropathy (CIPN) is a pervasive consequence of first-line anticancer agents (1,2). There are no drugs approved to prevent CIPN (1). First-line treatments for neuropathic pain include tricyclic antidepressants, serotonin/norepinephrine reuptake inhibitors, and antiepileptics, all of which exhibit modest efficacy or side effects (3). CIPN induced specifically by taxanes such as paclitaxel is resistant to such treatments (4).

Cannabis has been used for medicinal purposes to treat pain for centuries (5). However, Δ^9-tetrahydrocannabinol (THC), the major psychoactive ingredient in cannabis, produces equivocal results in people with neuropathic pain. In a recently published meta-analysis on cannabinoids and pain, efficacy was unclear due in part to formulation, different types of cannabinoids used, and route of administration (6). Inhaled cannabis was concluded to be more effective in relieving pain than oromucosal sprays with extracts of THC or THC/cannabidiol (CBD) (6). Smoked cannabis containing 9.4% THC suppressed numerical ratings of pain intensity in adults with posttraumatic or postsurgical neuropathic pain in a randomized, double-blind, placebo-controlled, 4-period crossover design evaluating 23 patients (7). In a pilot study of 16 subjects experiencing established CIPN, an oromucosal spray of nabiximols (Sativex whole cannabis extract) failed to reduce numerical ratings of pain intensity relative to placebo, although responder analysis revealed a subset of patients who benefited from nabiximols compared with placebo (8). The International Association for Study of Pain guidelines only weakly recommends the use of cannabinoids for the treatment of neuropathic pain (9). Concerns over small sample sizes, risk of bias, and inadequate blinding complicate interpretation of clinical trials evaluating efficacy of inhaled cannabis (10,11).

ISSN: 2451-9022

The clinical literature contrasts with results of rodent studies of CIPN that uniformly support the antinociceptive efficacy of cannabinoids such as THC (12–14) and the phytocannabinoid CBD (15–17) [for reviews, see (18,19)]. THC binds to CB_1 receptors in the brain, whereas CBD, which lacks these psychoactive properties, engages a myriad of diverse targets but shows little affinity for cannabinoid receptors [for a review, see (20)]. However, the validity of animal models of pathological pain has also been questioned (21).

Consequently, we used a preclinical brain imaging approach to evaluate the efficacy of inhalation of vaporized cannabis or placebo cannabis on established CIPN. We previously reported aberrant brain functional connectivity, including hyperconnectivity of the raphe nuclei, induced by the chemotherapeutic agent paclitaxel in rats, consistent with development of cold allodynia, a clinical symptom of CIPN (22). Behavioral and electrophysiological studies implicate a role for the raphe nuclei in cannabinoid analgesic mechanisms (23,24). Therefore, we hypothesized that THC-enriched cannabis would suppress CIPN and produce antinociception by decoupling the raphe nuclei.

METHODS AND MATERIALS

Animals

Male Sprague Dawley rats (300–325 g) were obtained from Charles River Laboratories (Wilmington, MA). Rats were maintained on a 12-hour light/dark cycle and allowed access to food and water ad libitum. Animal use followed the National Institutes of Health's Guide for the Care and Use of Laboratory Animals and adhered to the National Institutes of Health and American Association for Laboratory Animal Science guidelines. All protocols complied with the regulations of the Institutional Animal Care and Use Committee at Northeastern University and guidelines of the International Association for Study of Pain.

Drugs

Paclitaxel (Tecoland Corp., Irvine, CA) was dissolved in a vehicle consisting of Cremophor EL:ethanol:saline to achieve a final concentration of 1:1:18. Rats received either paclitaxel (2 mg/kg/day intraperitoneally [i.p.]; cumulative dose of 8 mg/kg i.p.) or its Cremophor-based vehicle 4 times on alternate days (i.e., days 0, 2, 4, and 6) using methods validated in our laboratories (13,25–31). We previously reported that paclitaxel-induced allodynia developed by day 7 postinjection and was maintained for at least 3 months using these methods (13,27,29,31). Experimenters were blinded to the experimental groups (i.e., paclitaxel vs. vehicle) during the measurements and analyses of cold sensitivity.

Active cannabis containing 10.3% THC but negligible CBD (0.05%) and placebo cannabis were provided by the National Institute on Drug Abuse through RTI International's NIDA Drug Supply Program. Cannabis was stored as dried minced marijuana plant at −20°C prior to use. Cannabis from each sample was vaporized in a Volcano (Storz & Bickel, Tuttlingen, Germany) using 460 mg of dry weight plant to achieve blood levels approximating 130 to 140 ng/mL (32). Vaporization heats the entire plant without igniting it, releasing phytocannabinoids into a vapor that is relatively free from the byproducts of combustion. The vapor was directly administered through a tube attached to a portal on a 26-quart small rodent holding box (22.00 inches long × 16.50 inches wide × 6.53 inches high) for 30 seconds. Rats were exposed to the vaporized cannabis for 30 minutes before performing behavioral or imaging experiments on separate days.

Cold Plate Assay

Responsiveness to cold stimulation was assessed using the cold plate assay (33), as we reported previously (22). Rats (n = 24) were acclimated to standing on a $^1/_4$ -inch glass plate table underneath a transparent plastic container (38 × 14 cm). A mirror permitted an unobstructed view of each rat's hindpaws for the precise placement of the cold probe. The plantar surface of the hindpaw was stimulated through the floor of the glass platform. The cold probe was tested on each hindpaw with a 7-minute interstimulation interval between each paw. Each hindpaw was tested 3 times with an interval of 15 minutes between trials. The latency to remove the hindpaw was timed in seconds using a 90-second cutoff latency. Withdrawal latencies were averaged across the right and left hindpaws to produce a single determination for each animal. Withdrawal latencies to cold stimulation were measured in all rats 5 days before paclitaxel or vehicle treatment to randomize the groups based on response times. Twenty-one days after cessation of treatment, rats were tested for cold allodynia. Testing post-treatment was done within 1 hour after exposure to vaporized THC cannabis or placebo. Because the behavior experiments for cold allodynia were a within-subjects design testing each rat following THC cannabis or placebo following paclitaxel or vehicle treatment, there was a washout period of at least 7 or 8 days between exposures (see Figure 1 for a schematic of

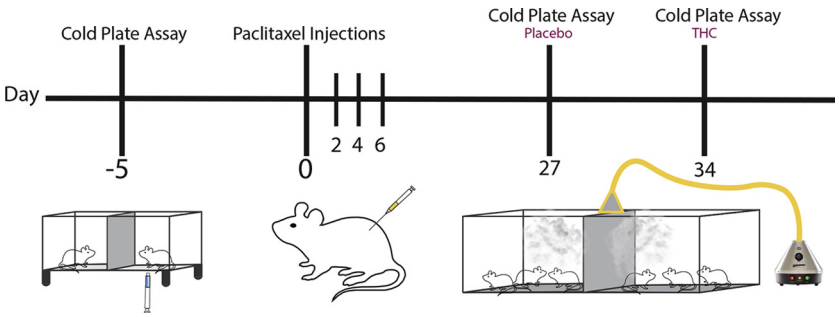

Figure 1. Experimental timeline. The schematic shows the timeline (days) of experimental steps taken to test for paclitaxel-induced cold allodynia with and without inhalation of vaporized THC cannabis or placebo. THC, Δ^9-tetrahydrocannabinol.

experimental steps). Two-way (2 × 3) analysis of variance, with chemotherapy status (paclitaxel vs. vehicle) as the between-subjects factor and vaporization treatment (prevaporization vs. THC cannabis vs. placebo cannabis) as the within-subjects factor, was followed by Tukey's post hoc tests. Simple effects, which control for number of comparisons using Tukey's multiple comparison test, were used to characterize the impact of the different vaporization conditions within each chemotherapy status group (i.e., paclitaxel vs. vehicle). Data were analyzed using GraphPad Prism 7.0 (GraphPad Software, La Jolla, CA).

Neuroimaging

Imaging sessions were conducted using a Bruker BioSpec 7.0T/20-cm USR magnet (Bruker, Billerica, MA). Radio frequency signals were sent and received with a quadrature volume coil built into the animal restrainer. The restraining system included a padded head support, obviating the need for ear bars to reduce animal discomfort while minimizing motion artifact. Rats (n = 7 paclitaxel; n = 6 vehicle) were imaged under 1% to 2% isoflurane while keeping a respiratory rate of 40 to 50 per minute. Imaging was performed 8 to 10 weeks after paclitaxel and vehicle treatments.

Resting-State Functional Connectivity

Scans were collected using a spin echo triple-shot echo-planar imaging sequence (imaging parameters: matrix size = 96 [height] × 96 [width] × 20 [diameter], repetition time/echo time = 1000/15 ms, voxel size = 0.312 × 0.312 × 1.2 mm, slice thickness = 1.2 mm, 200 repetitions, time of acquisition = 10 minutes). Benefits of multishot echo-planar imaging in blood oxygen level–dependent (BOLD) imaging were described previously (34–38). Preprocessing was accomplished by combining AFNI_17.1.12 (http://afni.nimh.nih.gov/afni/), FSL (version 5.0.9; http://fsl.fmrib.ox.ac.uk/fsl/), DRAMMS (Deformable Registration via Attribute Matching and Mutual-Saliency Weighting, version 1.4.1; https://www.cbica.upenn.edu/sbia/software/dramms/index.html), and MATLAB (The MathWorks, Natick, MA). Brain tissue masks for resting-state functional connectivity (rsFC) images were manually drawn using 3DSlicer (https://www.slicer.org/) and applied for skull stripping. There was a slice timing correction for the interleaved slice acquisition order. Normalization was completed by registering functional data to the 3D MRI Rat Brain Atlas (Ekam Solutions, Boston, MA) using affine registration through DRAMMS. The 3D MRI Rat Brain Atlas containing 171 annotated brain regions was used for segmentation. Data are reported in 166 brain areas (5 brain atlas regions were excluded from analysis owing to the large size of 3 brains). After quality assurance, bandpass filtering (0.01–0.1 Hz) was performed to reduce low-frequency drift effects and high-frequency physiological noise for each subject. The resulting images were further detrended and spatially smoothed (full width at half maximum = 0.8 mm). Finally, regressors composed of motion outliers, the 6 motion parameters, the mean white matter, and cerebrospinal fluid time series were fed into general linear models for nuisance regression to remove unwanted effects.

The region-to-region functional connectivity method was used to measure the correlations in spontaneous BOLD fluctuations. Voxel time series data were averaged in each node based on the residual images using the nuisance regression procedure. Pearson's correlation coefficients across all pairs of nodes (14,535 pairs) were computed for each subject. The r values (ranging from −1 to 1) were z transformed using the Fisher's z transform to improve normality. A 166 × 166 symmetric connectivity matrix was constructed for each experimental group. Group-level analysis was performed to look at the functional connectivity in the experimental groups. The resulting z-score matrices from one-group t tests were clustered using the k-nearest neighbors clustering method to identify how nodes cluster together and form resting-state networks. A z-score threshold of $|z|$ = 2.3 was applied to remove spurious or weak node connections for visualization purposes.

RESULTS

Vaporization of THC Suppresses Paclitaxel-Induced Cold Allodynia

Paclitaxel treatment reduced paw withdrawal latencies to cold stimulation relative to vehicle treatment (chemotherapy status:

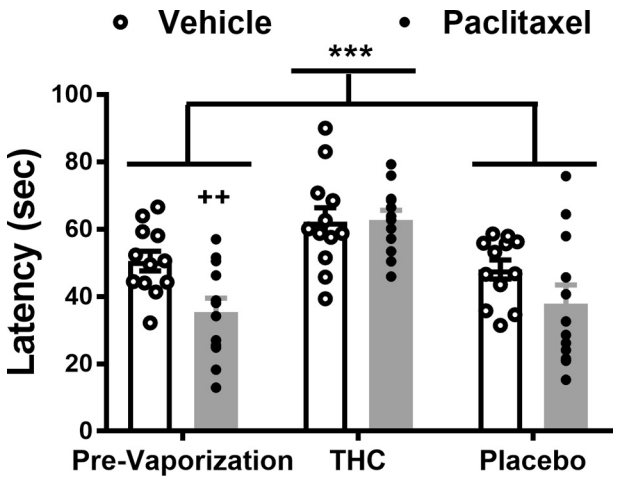

Figure 2. Paclitaxel decreases, whereas vaporized THC-enriched cannabis increases, paw withdrawal latencies to cold stimulation. Inhalation of vaporized cannabis containing THC increases paw withdrawal latencies to cold stimulation. Paw withdrawal latencies to cold stimulation were lower in paclitaxel-treated rats compared with vehicle-treated rats, consistent with development of cold allodynia induced by chemotherapy ($F_{1,22}$ = 5.385, p = .0300). Paw withdrawal latencies were higher following vaporization of THC cannabis compared with placebo cannabis or prevaporization responding irrespective of chemotherapy status ($F_{2,44}$ = 19.76, $p < .0001$). Simple-effects analysis revealed that in paclitaxel-treated rats, paw withdrawal latencies were higher following vaporization of THC-enriched cannabis relative to prevaporization levels ($p < .0001$, Tukey's multiple comparison test) and vaporization of placebo cannabis ($p < .0001$, Tukey's multiple comparison test). In vehicle-treated rats, paw withdrawal latencies were higher following vaporization of THC cannabis compared with placebo cannabis (p = .0203, Tukey's multiple comparison test) but not compared with prevaporization responding (p = .0659, Tukey's multiple comparison test). Individual subjects' responding is shown by the scatter plot. Data are mean ± SEM. ***$p < .0001$ vs. prevaporization and placebo (two-way [2 × 3] analysis of variance followed by Tukey's post hoc test). Prior to vaporization, paclitaxel reduced cold withdrawal latencies relative to vehicle treatment (t_{22} = 3.026, p = .0032 vs. vehicle treatment). $^{++}p < .01$, unpaired t test, one tailed. THC, Δ^9-tetrahydrocannabinol.

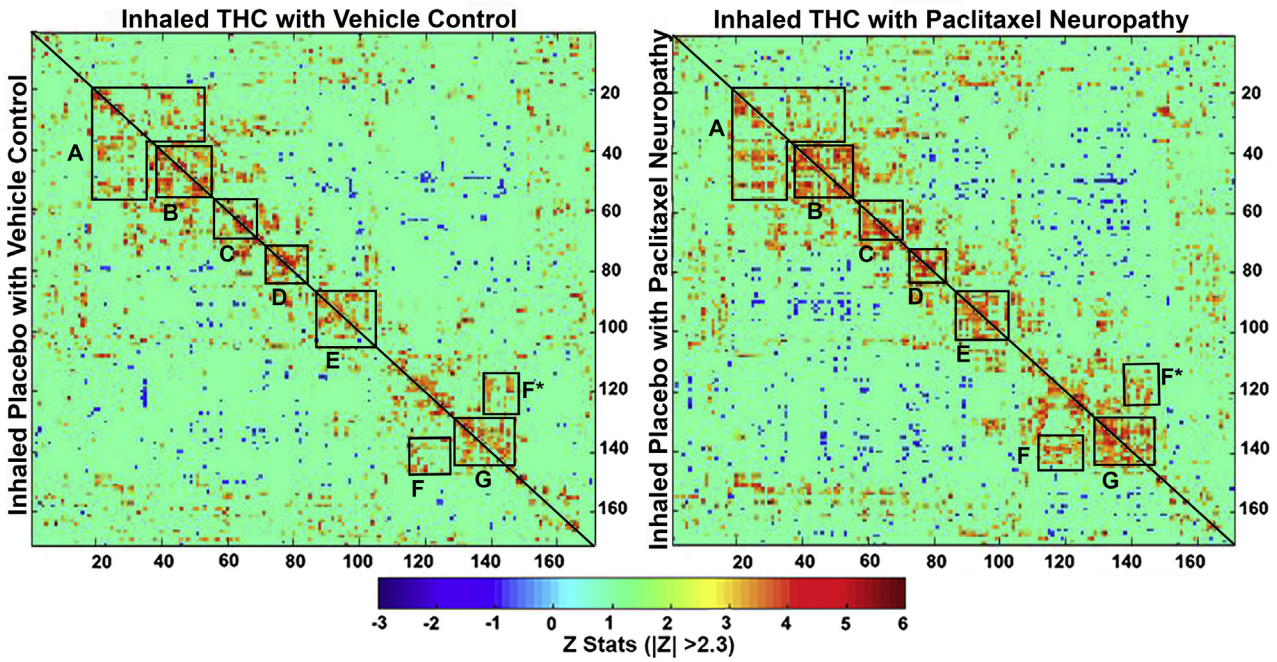

Figure 3. Resting-state functional connectivity. The left correlation matrix compares functional coupling between rats treated with vehicle and later exposed to inhaled vaporized cannabis plant high in THC or placebo. The right matrix compares connectivity between rats treated with paclitaxel to induce cold allodynia and later treated with inhaled placebo or THC. The diagonal line in each matrix separates the two experimental conditions. Each colored red/orange pixel represents 1 of 166 brain areas that has a significant positive correlation with other brain areas. Pixels in shades of blue have a significant negative correlation, or anticorrelation, with other brain regions. The brain areas with significant correlations appear as clusters because they are contiguous in their neuroanatomy and function. Each pixel on one side of the line has a mirror image pixel on the other side. The delineated areas serve to focus attention on similarities and differences in connectivity. Areas: **(A)** prefrontal cortex (e.g., orbital, prelimbic, infralimbic, and anterior cingulate cortices connections with accumbens, ventral pallidum, basal ganglia, and central amygdala); **(B)** basal ganglia/hypothalamus/amygdala; **(C)** thalamus; **(D)** thalamus/hippocampus; **(E)** pons/midbrain; **(F)** cerebellum/brainstem; **(G)** cerebellum. THC, Δ^9-tetrahydrocannabinol.

$F_{1,22}$ = 5.385, p = .03), vaporization differentially altered paw withdrawal latencies (vaporization treatment: $F_{2,44}$ = 19.76, $p <$ .0001), and the interaction between chemotherapy status and vaporization treatment was not significant ($F_{2,44}$ = 2.48, p = .0954) (Figure 2). Tukey's post hoc test revealed that vaporization of THC-enriched cannabis increased cold withdrawal latencies relative to either prevaporization latencies ($p <$ .0001) or vaporization of placebo cannabis ($p <$ .0001). Prevaporization responsiveness to cold did not differ from responsiveness assessed following vaporization of placebo cannabis (p = .9998).

Simple effects were also used to compare the impact of each vaporization condition within each chemotherapy status group (i.e., paclitaxel vs. vehicle) using Tukey's multiple comparison tests. In paclitaxel-treated rats, vaporization of THC-enriched cannabis increased cold withdrawal latencies relative to either prevaporization responsiveness ($p <$ .0001) or vaporization of placebo cannabis ($p <$ .0001). In vehicle-treated rats, vaporization of THC-enriched cannabis increased cold withdrawal latencies relative to placebo cannabis (p = .0203) but not relative to prevaporization responding (p = .0659). Cold withdrawal latencies did not differ between prevaporization responding and placebo cannabis within either the paclitaxel-treated groups (p = .8856) or the vehicle-treated groups (p = .8729). Thus, vaporization of THC-enriched cannabis suppressed paclitaxel-induced cold allodynia while also producing antinociception in vehicle-treated animals.

Resting-State Functional Connectivity

Rats were tested for rsFC when paclitaxel-induced allodynia remained stable, that is, at 2 months following initiation of paclitaxel dosing (27). Prior to testing, rats were exposed to inhaled vaporized cannabis plant for 30 minutes. These data were collected within 50 to 60 minutes of exposure under light isoflurane anesthesia. Figure 3 shows two correlation matrices comparing 166 brain areas for rsFC between the vehicle condition exposed to inhaled placebo or THC (left matrix) and the paclitaxel condition exposed to placebo or THC. The delineated areas serve to focus attention on similarities and differences in connectivity. Comparison of correlation matrices revealed that paclitaxel-treated rats have greater positive and negative connectivity compared with vehicle-treated rats. For example, area A includes most of the brain areas comprising the prefrontal cortex, basal ganglia, and some amygdala regions (e.g., orbital, prelimbic, infralimbic, motor, and anterior cingulate cortices, accumbens, ventral pallidum, central amygdala, septum). These areas are associated with emotion, motivation, and executive

Table 1. Connections With the Dorsal Raphe

Placebo	*z* Value	THC	*z* Value
Control			
Claustrum	−2.79	2nd Cerebellar lobule	2.37
Lemniscal nucleus	2.41	Anterior pretectal nucleus	2.52
2nd Cerebellar lobule	2.42	Median raphe	2.71
Pontine reticular nucleus	2.54	Reticular nucleus midbrain	2.77
CA2	2.55	Dorsomedial tegmentum	2.79
CA3 dorsal	2.61	Inferior colliculus	3.21
Central gray	2.76	Precuniform nucleus	3.40
Periaqueductal gray	2.80	Periaqueductal gray	3.41
10th Cerebellar lobule	2.83		
Paclitaxel			
Crus 1 of ansiform lobule	−3.11	Paraventricular thalamus	−3.12
Ventral medial striatum	−3.04	Central medial thalamus	−2.43
Mag preoptic nucleus	−2.96	Anterior olfactory nucleus	−2.33
Paramedian lobule	−2.72	Gigantocellular reticularis	2.32
Accumbens core	−2.70	Cochlear nucleus	2.38
Crus 2 of ansiform lobule	−2.58	Reticular nucleus midbrain	2.40
Root of trigeminal nerve	−2.56	Parabrachial nucleus	2.41
Globus pallidus	−2.38	Periaqueductal gray	2.53
Olfactory tubercles	−2.30	Sub nigra compacta	2.63
Motor trigeminal nucleus	2.33	Facial nucleus	3.01
Sub coeruleus nucleus	2.33	2nd Cerebellar lobule	3.62
Ectorhinal cortex	2.36		
Subiculum dorsal	2.38		
Dorsomedial tegmentum	2.42		
CA1 dorsal	2.45		
Inferior colliculus	2.56		
Entorhinal cortex	2.59		
Superior colliculus	2.64		
Retrosplenial caudal cortex	2.76		
Reticular nucleus midbrain	2.78		
Central gray	3.05		
2nd Cerebellar lobule	3.05		
Medial mammillary nucleus	3.26		
Periaqueductal gray	3.41		
3rd Cerebellar lobule	4.53		

Mag, magnocellular; Sub, substantia; THC, Δ9-tetrahydrocannabinol.

control. Note that for both conditions THC vapor exposure reduces connectivity, particularly in the paclitaxel-treated rats. The precise *z* values for correlations between all 166 brains areas for each experimental condition are provided in the Supplement.

Table 1 lists the brain areas and their *z* scores for each experimental condition with significant positive and negative connectivity to the dorsal raphe. Negative connectivity is highlighted in blue. Vehicle-treated rats exposed to vaporized placebo or THC are similar in the number of functionally coupled areas. Exposure to paclitaxel greatly enhanced both negative and positive coupling, which was reduced with vaporized THC but not with placebo. The location of the brain areas in Table 1 are shown as 2D heat maps for each experimental condition in Figure 4. In vehicle-treated rats exposed to vaporized placebo, positive functional connectivity (highlighted in red) was limited to the adjacent periaqueductal gray (PAG), CA3, and CA2 of the hippocampus (Figure 4B) and the second cerebellar lobule, central gray, and pontine reticular nucleus (Figure 4D). Vehicle-treated rats exposed to vaporized THC showed increase functional coupling to adjacent areas such as the reticular nucleus of the midbrain, anterior pretectal area, PAG (Figure 4B), precuniform nucleus, and median raphe (Figure 4C). Positive connectivity extended caudally to include the inferior colliculus, second cerebellar lobule, and dorsal tegmental area (Figure 4D). Like the PAG, the dorsal raphe showed several areas of anti-correlation (highlighted in blue) in paclitaxel-treated rats exposed to vaporized placebo. The most rostral areas included the ventral medial striatum, accumbens core, and olfactory tubercles (Figure 4A), all of which have afferent dopaminergic connections with the ventral tegmental area. The most caudal areas included the crus 1 and crus 2 ansiform, paramedian lobules of the cerebellum, and root of the trigeminal nerve (Figure 4F). Conversely, this same experimental condition showed extensive positive functional coupling between the dorsal raphe and PAG, CA1, reticular nucleus, retrosplenial and entorhinal cortices (Figure 4B), superior and inferior colliculi, subiculum, first and third cerebellar lobules, ectorhinal cortex, motor trigeminal nerve, and sub coeruleus (Figure 4C–E). Paclitaxel-treated rats exposed to vaporized THC showed a pronounced reduction in both positive and negative connectivity. These brain areas for paclitaxel treatment with and without vaporized THC are summarized as color-coded 3D volumes below.

Table 2 lists brain areas and their *z* scores for each experimental condition with significant positive and negative connectivity to the median raphe. Vehicle treatment with or without THC exposure shows only a modest number of significant connections, while rats treated with paclitaxel plus placebo show hyperconnectivity that was diminished with THC exposure. The anatomical organization of these brain areas for each experimental condition is shown in Figure 5. In vehicle-treated rats subjected to vaporization of placebo or THC-enriched cannabis, only a modest coupling of raphe to surrounding areas was observed. THC-enriched cannabis exposure uncouples the raphe from the PAG. The difference between paclitaxel-treated rats subjected to vaporization of THC-enriched cannabis and those subjected to placebo cannabis is stark. Paclitaxel-treated rats subjected to placebo vaporization show extensive coupling of the raphe with visual, temporal, retrosplenial, and entorhinal cortices, inferior and superior colliculi, cerebellum, and several areas that comprise the ascending reticular activating system (e.g., midbrain reticular system, pontine and pedunculopontine reticular areas, sensory trigeminal nucleus). Exposure to THC-enriched vapor essentially uncoupled all these areas. The fingerprints of coupling with the raphe induced by vaporization of THC-enriched cannabis in either the presence or absence of paclitaxel are nearly identical (*z* values in Table 2). Note that the few negatively correlated brain

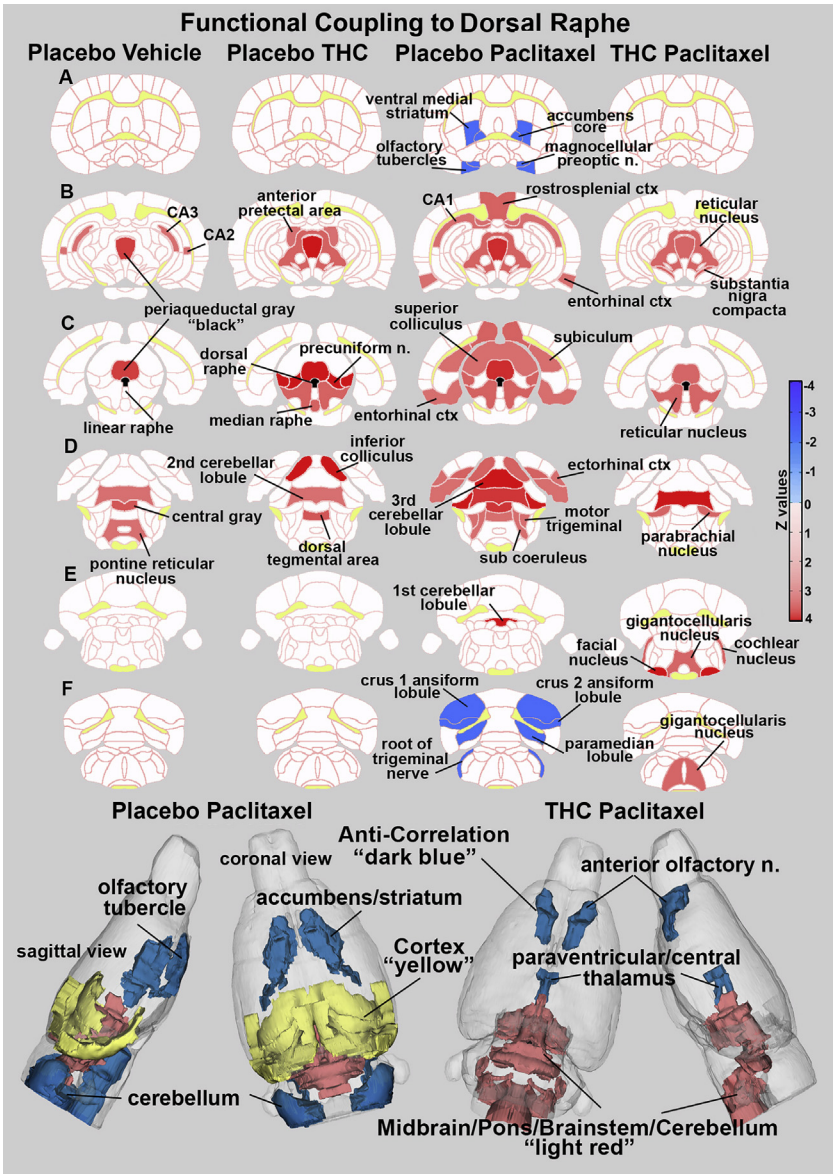

Figure 4. Functional coupling to the dorsal raphe. Paclitaxel produces hyperconnectivity of functional coupling to the dorsal raphe that is attenuated by vaporization of THC-enriched cannabis. The columns of 2D images show heat maps of significant connectivity (*z* values) for each experimental condition. The shades of red (positive connectivity) and blue (negative connectivity) appear on anatomical sections taken from the rat brain atlas. These sections are identical across rows **(A–F)**. Yellow highlights white matter tracts, and black shows the location of the dorsal raphe in **(C)**. The brain areas with significant connectivity to the dorsal raphe were taken from Table 1. The most rostral brain areas in Table 1 (e.g., anterior olfactory nucleus) are not shown in these 2D sections but are displayed in the 3D color-coded reconstruction of the placebo paclitaxel and THC paclitaxel conditions below. ctx, cortex; n., nucleus; THC, Δ^9-tetrahydrocannabinol.

areas listed in Table 2 were not represented in the 2D heat maps but are shown in the 3D reconstructions (e.g., medial septum, central medial thalamus, frontal association cortex, dorsal lateral striatum, tenth cerebellar lobule).

DISCUSSION

To our knowledge, the current study is the first—animal or human—to evaluate the impact of inhaled vaporized THC-enriched cannabis on neuropathic nociception or changes in brain rsFC induced by pathological pain. Vaporized cannabis used here contained 10.3% THC but negligible (0.05%) CBD. Inhalation of THC-enriched cannabis suppressed paclitaxel-induced cold allodynia and normalized brain rsFC induced by chemotherapy treatment. We previously reported reorganization of brain nociceptive neuronal circuitry following paclitaxel treatment; our findings suggested that increased connectivity of the median raphe could be a neuroadaptive response contributing to CIPN (22). Here, inhalation of THC-enriched cannabis dramatically reduced the coupling of the raphe in paclitaxel-treated rats under conditions in which paclitaxel-induced neuropathic nociception was also suppressed. These effects were absent following vaporization of placebo cannabis. Our preclinical neuroimaging experiments frame both the animal and clinical literature on efficacy of cannabis for treating neuropathic pain. Notably, THC-enriched cannabis also produced antinociception in vehicle-treated rats under these conditions.

Table 2. Connections With the Median Raphe

Placebo	*z* Value	THC	*z* Value
	Control		
Anterior cingulate cortex	−2.42	Medial dorsal thalamus	−2.53
Dorsomedial tegmental area	2.50	Ventromedial thalamus	−2.46
Raphe linear	2.73	Central gray	2.40
Reticulotegmental nucleus	2.77	Interpeduncular nucleus	2.49
Interpeduncular nucleus	2.91	Anterior pretectal nucleus	2.49
Pon reticular nucleus oral	3.21	Dorsal raphe	2.71
Periaqueductal gray	3.73	Pon reticular nucleus oral	2.86
		Dorsomedial teg area	3.11
		Raphe linear	3.36
	Paclitaxel		
Medial septum	−3.23	Frontal association cortex	−2.91
Central medial thalamus	−2.54	Dorsal lateral striatum	−2.46
Entorhinal cortex	2.35	10th Cerebellar lobule	−2.42
Pon reticular nucleus caudal	2.41	Flocculus cerebellum	2.40
Ventral tegmental area	2.43	Anterior lobe pituitary	2.52
Pedunculopontine tegmentum	2.45	Central gray	2.64
Raphe magnus	2.49	Reticulotegmental nucleus	2.96
Precuniform nucleus	2.56	Interpeduncular nucleus	3.06
Retrosplenial cortex	2.57	Pon reticular nucleus oral	3.15
Lemniscal nucleus	2.59	Dorsomedial tegmentum	3.32
Anterior pretectal nucleus	2.62	Raphe linear	3.89
Principal sensory nucleus trig	2.79		
Inferior colliculus	2.82		
Reticulotegmental nucleus	2.90		
Central gray	2.91		
Visual 2 cortex	2.91		
Temporal cortex	2.93		
Ectorhinal cortex	2.95		
Pon reticular nucleus oral	3.01		
2nd Cerebellar lobule	3.05		
Visual 1 cortex	3.14		
3rd Cerebellar lobule	3.16		
Reticular nucleus midbrain	3.23		
Superior colliculus	3.40		
Raphe linear	3.46		
Dorsomedial tegmentum	3.55		
Interpeduncular nucleus	3.62		

Pon, pontine; teg, tegmental; THC, Δ9-tetrahydrocannabinol; trig, trigeminal.

Preclinical Studies in Animals

THC administered i.p. suppresses neuropathic pain behavior, including CIPN produced by paclitaxel (12) and cisplatin (39) in rodents. Inhaled vaporized THC cannabis produces antinociception in a test of acute nociception, the tail withdrawal assay, in both mice (40) and rats (41,42), effects attributable to THC acting on CB_1 receptors (43–45). THC administered i.p. also suppresses nociception in models of inflammatory pain (46,47), traumatic nerve injury (48,49), arthritis (50), and diabetic neuropathy (51) and produces synergistic antiallodynic effects with conventional analgesics (52). Our studies corroborate the general antinociceptive effect of THC. However, none of the preclinical studies noted above evaluated inhaled THC from cannabis, mimicking conditions employed by people.

Vaporization of THC-enriched cannabis suppressed paclitaxel-induced allodynia and uncoupled the dorsal and median raphe, normalizing brain rsFC to levels observed following vehicle treatment. The raphe nuclei are noted for their rich populations of serotonergic neurons, and serotonergic hyperactivity in the raphe contributes to neuropathic pain (53). Spinal nerve ligation produces serotonergic hyperactivity and increased levels of extracellular serotonin in the dorsal raphe in rats (53), whereas WIN 55,212-2, a pan cannabinoid agonist, restores normal serotoninergic function and reverses nerve injury–induced hyperalgesia and allodynia (53). Changes in endocannabinoid tone have also been detected in the dorsal raphe following chronic constriction injury (54). More work is necessary to determine whether CBD in cannabis could enhance efficacy and/or attenuate unwanted side effects (e.g., psychoactivity, tolerance) induced by THC.

Clinical Studies

A Cochrane review concluded that there is no high-quality evidence for the efficacy of any cannabis-based product in any chronic neuropathic pain condition, but it noted that efficacy may differ by product and type of pain (55). An individual patient data meta-analysis of 178 participants reported that inhaled cannabis was effective in the short term for 1 in 5 or 6 patients experiencing neuropathic pain associated with HIV, diabetes, or nerve injury (56). However, inhaled cannabinoids have not been tested in patients with CIPN (6). Nabiximols, a full-spectrum cannabis extract used as an oromucosal spray, had no overall effect on numerical ratings of pain intensity in a double-blind, placebo-controlled exploratory study with 18 patients who received paclitaxel, vincristine, or cisplatin (8). Nonetheless, even in this underpowered pilot trial, responder analysis identified a subset of patients who exhibited significant reductions of numerical ratings of pain intensity scores relative to the placebo arm of the same subjects (8). While dronabinol, a purified oral THC, is ineffective in treating neuropathic pain associated with multiple sclerosis (57), nabiximols was suggested to be effective in treating multiple sclerosis–induced hyperalgesia and allodynia (58–60). We specifically chose to study inhaled cannabis to enhance translational relevance and because modest analgesic efficacy is supported for this route of administration [e.g., (61,62)]. By contrast, oral administration of synthetic cannabinoids has largely failed to show efficacy in randomized controlled trials (6).

Functional Imaging Studies

We know of only one clinical study that used imaging to evaluate the effect of cannabinoids on neuropathic pain. Patients with chronic neuropathic lower limb pain were imaged for changes in rsFC using the anterior cingulate as a seed; sublingual THC administration reduced connectivity to the sensorimotor cortex that covaried with a subjective pain rating (63). However, the mesencephalic and brainstem regions that include the PAG and raphe were not studied. Hence, to our knowledge, the current study is the only one—human or

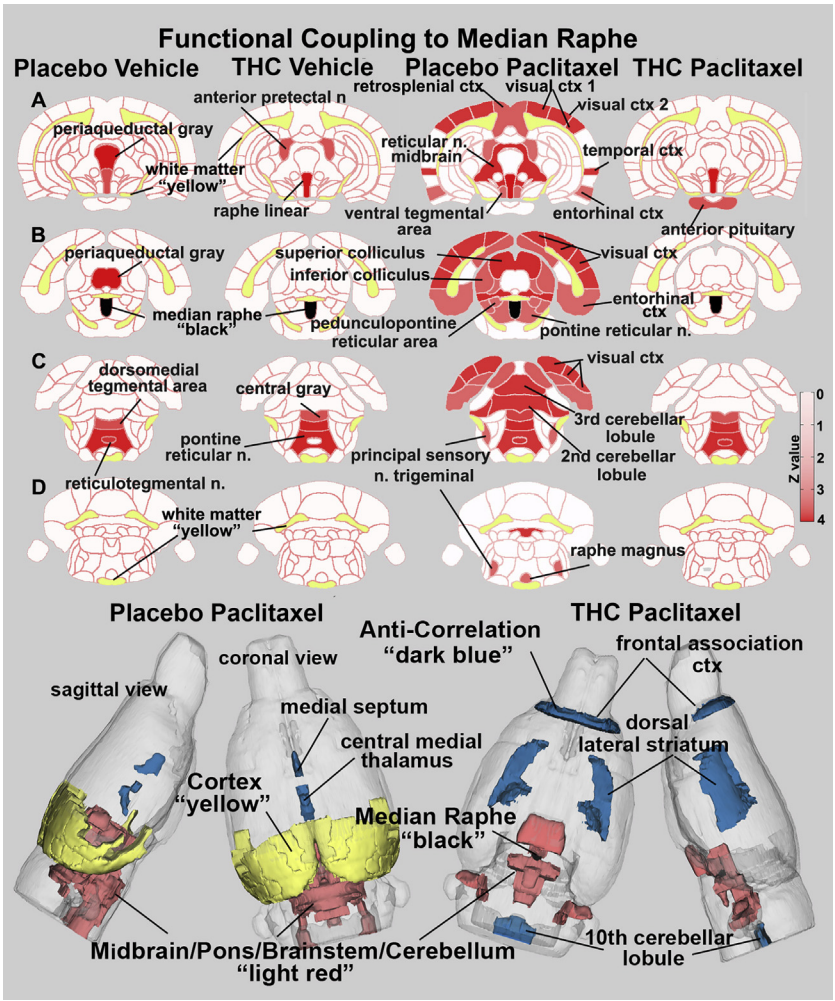

Figure 5. Functional coupling to the median raphe. Paclitaxel produces hyperconnectivity of functional coupling to the median raphe that is attenuated by vaporization of THC-enriched cannabis. The columns of 2D images show heat maps of significant connectivity (*z* values) for each experimental condition. The shades of red (positive connectivity) appear on anatomical sections taken from the rat brain atlas. These sections are identical across rows **(A–D)**. Yellow highlights white matter tracts, and black shows the location of the median raphe in **(B)**. The brain areas with significant connectivity to the median raphe were taken from Table 2. The most rostral and caudal brain areas showing negative coupling in Table 2 do not appear in the 2D images but are shown in blue in the color-coded 3D reconstruction of placebo paclitaxel and THC paclitaxel conditions below. ctx, cortex; n., nucleus; THC, Δ^9-tetrahydrocannabinol.

animal—that has evaluated the impact of inhaled THC on rsFC in neuropathic pain.

Modulation of pain neural circuitry via ascending and descending pathways that influence the sensory and affective components of neuropathy is exacerbated by serotonin neurotransmission (64,65), whereas facilitation of neuropathic pain is dependent on the type of serotonin receptor engaged (66–68). Here, we showed that the neuroadaptation to paclitaxel treatment and CIPN is hyperconnectivity in the midbrain raphe nuclei. CB_1 receptors, the endogenous cannabinoid receptors and targets of THC, are localized to these nuclei (69,70), and analgesic effects of cannabinoids are dependent on the rostral ventromedial medulla (24). Activation of CB_1 with THC or the agonist WIN 55,212-2 inhibits serotonin levels in brain regions with afferent connections to the midbrain raphe nuclei (71–73). Conversely, blocking the CB_1 receptor enhances release of serotonin (74,75). The reduced functional coupling of the raphe nuclei following inhaled THC is consistent with the literature and may underlie the antinociceptive effects observed here.

Limitations and Considerations

The historical status of cannabis as an illicit or recently licit drug, together with variability in material/biochemical content and lack of large-scale, randomized, controlled clinical trials, has complicated interpretation of its therapeutic potential [for a review, see (5)]. Psychoactive effects and potential for abuse limit both research efforts and clinical use (5). Our studies suggest that vaporization of THC-enriched cannabis suppresses chemotherapy-induced neuropathic allodynia and normalizes paclitaxel-induced changes in brain rsFC in brain regions associated with nociceptive processing and also produces antinociception (22). Several limitations of the current study should be noted. First, the cannabis plant has numerous bioactive phytocannabinoids and terpenes that could contribute to the current findings. Second, THC-enriched cannabis was vaporized as an acute exposure of a single THC concentration during the maintenance phase of paclitaxel-induced neuropathy. Repeated exposure to THC could potentially result in tolerance to therapeutic benefit, as we observed previously in paclitaxel-treated mice receiving

THC i.p. (12). Third, our study did not address whether vaporization of THC-enriched cannabis, administered prophylactically, would block the development of neuropathic nociception. Fourth, sex, age, or pharmacokinetic differences in responses to THC can be observed (76–80), but only male rats were tested in the current study. Fifth, rats were lightly anesthetized with isoflurane to minimize motion and physiological stress during resting-state BOLD functional connectivity imaging [for a review, see (81)]. Anesthesia may reduce the magnitude of the BOLD signal but does not disrupt the connectivity, as demonstrated across species and under different physiological conditions (82–86). However, activation of the dorsal raphe and the subsequent increase in serotonergic neurotransmission is linked to arousal and recovery from isoflurane anesthesia (87). Thus, when interpreting the data, one cannot exclude the possibility that exposure to light isoflurane during the imaging session was reducing serotonin release in all four experimental conditions. However, anesthetic treatment and use of a head cradle for rsFC measurements were identical for all groups, and yet the effects of vaporization of THC-enriched cannabis versus placebo cannabis were markedly distinct in paclitaxel- and vehicle-treated rats. Thus, exposure to isoflurane alone cannot explain the pattern of results obtained here.

Conclusions

The current study is the first to show that inhalation of vaporized THC-enriched cannabis suppresses neuropathic nociception in CIPN and also produces antinociception. Use of inhaled THC enhances the clinical relevance of our findings in the context of an emerging clinical literature suggesting that intrapulmonary exposure may be more effective in suppressing pain compared with other routes of administration (6). Assessments of rsFC identified key nodes in nociceptive neural circuitry most affected by cannabis vaporization. Strikingly, both the dorsal raphe and median raphe were uncoupled by vaporization of THC-enriched cannabis, suggesting a previously unrecognized role for this circuitry in the maintenance of CIPN. A preclinical imaging approach may compensate for limitations of existing animal models of CIPN (i.e., that rely extensively on measures of evoked pain) as well as limitations of clinical trials of inhaled cannabis (i.e., where inadequate blinding and small sample sizes may complicate interpretation) and may help to guide future clinical trials of efficacy of cannabinoids to the most appropriate therapeutic indications.

ACKNOWLEDGMENTS AND DISCLOSURES

This work was supported by National Institutes of Health (Grant Nos. DA047858, DA041229, and CA200417 [to AGH]) and a Grant Linking University Wide Expertise from the Indiana Clinical Translational Sciences Institute. Support was provided in part by a Howard Hughes Medical Institute–funded Inclusive Excellence Award to Northeastern University (principal investigator, Mary Jo Ondrechen).

All the authors contributed substantially to the manuscript. Concept, drafting and interpretation: CFF, AGH, IA, ARM. Execution: PK, XC, IA, ARM, AHS. Analysis: PK, XC, IA, ARM, AHS, AGH, CFF.

We thank the National Institute on Drug Abuse and RTI International for the cannabis extracts.

CFF has a financial interest in Animal Imaging Research, the company that makes the RF electronics and holders for animal imaging. All other authors report no biomedical financial interests or potential conflicts of interest.

ARTICLE INFORMATION

From the Center for Translational Neuroimaging (IA, ARM, AHS, XC, PK, CFF) and Department of Psychology (CFF), Northeastern University, Boston, Massachusetts; and Psychological and Brain Sciences (AGH), Program in Neuroscience, and Gill Center for Biomolecular Science, Indiana University, Bloomington, Indiana.

Address correspondence to Craig F. Ferris, Ph.D., at c.ferris@northeastern.edu.

Received Aug 20, 2020; revised Oct 30, 2020; accepted Nov 22, 2020.

Supplementary material cited in this article is available online at https://doi.org/10.1016/j.bpsc.2020.11.015.

REFERENCES

1. Ibrahim EY, Ehrlich BE (2020): Prevention of chemotherapy-induced peripheral neuropathy: A review of recent findings. Crit Rev Oncol Hematol 145:102831.
2. Seretny M, Currie GL, Sena ES, Ramnarine S, Grant R, MacLeod MR, *et al.* (2014): Incidence, prevalence, and predictors of chemotherapy-induced peripheral neuropathy: A systematic review and meta-analysis. Pain 155:2461–2470.
3. Szok D, Tajti J, Nyari A, Vecsei L (2019): Therapeutic approaches for peripheral and central neuropathic pain. Behav Neurol 2019:8685954.
4. Smith EM, Pang H, Cirrincione C, Fleishman S, Paskett ED, Ahles T, *et al.* (2013): Effect of duloxetine on pain, function, and quality of life among patients with chemotherapy-induced painful peripheral neuropathy: A randomized clinical trial. JAMA 309:1359–1367.
5. Russo EB (2008): Cannabinoids in the management of difficult to treat pain. Ther Clin Risk Manag 4:245–259.
6. Rabgay K, Waranuch N, Chaiyakunapruk N, Sawangjit R, Ingkaninan K, Dilokthornsakul P (2020): The effects of cannabis, cannabinoids, and their administration routes on pain control efficacy and safety: A systematic review and network meta-analysis. J Am Pharm Assoc 60:225–234.e6.
7. Ware MA, Wang T, Shapiro S, Robinson A, Ducruet T, Huynh T, *et al.* (2010): Smoked cannabis for chronic neuropathic pain: A randomized controlled trial. CMAJ 182:E694–E701.
8. Lynch ME, Cesar-Rittenberg P, Hohmann AG (2014): A double-blind, placebo-controlled, crossover pilot trial with extension using an oral mucosal cannabinoid extract for treatment of chemotherapy-induced neuropathic pain. J Pain Symptom Manage 47:166–173.
9. Finnerup N (2014): Treatment of neuropathic pain: Opioids, cannabinoids, and topical agents. In: Srinivasa N, Raja CLS, editors. Pain 2014 Refresher Courses: 15th World Congress on Pain. Washington, DC: IASP Press, 239–245.
10. Fisher E, Eccleston C, Degenhardt L, Finn DP, Finnerup NB, Gilron I, *et al.* (2019): Cannabinoids, cannabis, and cannabis-based medicine for pain management: A protocol for an overview of systematic reviews and a systematic review of randomised controlled trials. Pain Rep 4:e741.
11. Hauser W, Finnerup NB, Moore RA (2018): Systematic reviews with meta-analysis on cannabis-based medicines for chronic pain: A methodological and political minefield. Pain 159:1906–1907.
12. Deng L, Guindon J, Cornett BL, Makriyannis A, Mackie K, Hohmann AG (2015): Chronic cannabinoid receptor 2 activation reverses paclitaxel neuropathy without tolerance or cannabinoid receptor 1-dependent withdrawal. Biol Psychiatry 77:475–487.
13. Rahn EJ, Deng L, Thakur GA, Vemuri K, Zvonok AM, Lai YY, *et al.* (2014): Prophylactic cannabinoid administration blocks the development of paclitaxel-induced neuropathic nociception during analgesic treatment and following cessation of drug delivery. Mol Pain 10:27.
14. Rahn EJ, Makriyannis A, Hohmann AG (2007): Activation of cannabinoid CB1 and CB2 receptors suppresses neuropathic nociception evoked by the chemotherapeutic agent vincristine in rats. Br J Pharmacol 152:765–777.

15. Deng L, Cornett BL, Mackie K, Hohmann AG (2015): CB1 Knockout mice unveil sustained CB2-mediated antiallodynic effects of the mixed CB1/CB2 agonist CP55,940 in a mouse model of paclitaxel-induced neuropathic pain. Mol Pharmacol 88:64–74.
16. King KM, Myers AM, Soroka-Monzo AJ, Tuma RF, Tallarida RJ, Walker EA, *et al.* (2017): Single and combined effects of Δ^9-tetrahydrocannabinol and cannabidiol in a mouse model of chemotherapy-induced neuropathic pain. Br J Pharmacol 174:2832–2841.
17. De Gregorio D, McLaughlin RJ, Posa L, Ochoa-Sanchez R, Enns J, Lopez-Canul M, *et al.* (2019): Cannabidiol modulates serotonergic transmission and reverses both allodynia and anxiety-like behavior in a model of neuropathic pain. Pain 160:136–150.
18. Blanton HL, Brelsfoard J, DeTurk N, Pruitt K, Narasimhan M, Morgan DJ, *et al.* (2019): Cannabinoids: Current and future options to treat chronic and chemotherapy-induced neuropathic pain. Drugs 79:969–995.
19. Rahn EJ, Hohmann AG (2009): Cannabinoids as pharmacotherapies for neuropathic pain: From the bench to the bedside. Neurotherapeutics 6:713–737.
20. Russo EB (2017): Cannabidiol claims and misconceptions. Trends Pharmacol Sci 38:198–201.
21. Berge OG (2011): Predictive validity of behavioural animal models for chronic pain. Br J Pharmacol 164:1195–1206.
22. Ferris CF, Nodine S, Pottala T, Cai X, Knox TM, Fofana FH, *et al.* (2019): Alterations in brain neurocircuitry following treatment with the chemotherapeutic agent paclitaxel in rats. Neurobiol Pain 6:100034.
23. Martin WJ, Tsou K, Walker JM (1998): Cannabinoid receptor-mediated inhibition of the rat tail-flick reflex after microinjection into the rostral ventromedial medulla. Neurosci Lett 242:33–36.
24. Meng ID, Manning BH, Martin WJ, Fields HL (1998): An analgesia circuit activated by cannabinoids. Nature 395:381–383.
25. Carey LM, Lee WH, Gutierrez T, Kulkarni PM, Thakur GA, Lai YY, *et al.* (2017): Small molecule inhibitors of PSD95-nNOS protein-protein interactions suppress formalin-evoked Fos protein expression and nociceptive behavior in rats. Neuroscience 349:303–317.
26. Deng L, Guindon J, Vemuri VK, Thakur GA, White FA, Makriyannis A, *et al.* (2012): The maintenance of cisplatin- and paclitaxel-induced mechanical and cold allodynia is suppressed by cannabinoid CB_2 receptor activation and independent of CXCR4 signaling in models of chemotherapy-induced peripheral neuropathy. Mol Pain 8:71.
27. Deng L, Lee WH, Xu Z, Makriyannis A, Hohmann AG (2016): Prophylactic treatment with the tricyclic antidepressant desipramine prevents development of paclitaxel-induced neuropathic pain through activation of endogenous analgesic systems. Pharmacol Res 114:75–89.
28. Lee WH, Xu Z, Ashpole NM, Hudmon A, Kulkarni PM, Thakur GA, *et al.* (2015): Small molecule inhibitors of PSD95-nNOS protein-protein interactions as novel analgesics. Neuropharmacology 97:464–475.
29. Panoz-Brown D, Carey LM, Smith AE, Gentry M, Sluka CM, Corbin HE, *et al.* (2017): The chemotherapeutic agent paclitaxel selectively impairs reversal learning while sparing prior learning, new learning and episodic memory. Neurobiol Learn Mem 144:259–270.
30. Rahn EJ, Zvonok AM, Thakur GA, Khanolkar AD, Makriyannis A, Hohmann AG (2008): Selective activation of cannabinoid CB2 receptors suppresses neuropathic nociception induced by treatment with the chemotherapeutic agent paclitaxel in rats. J Pharmacol Exp Ther 327:584–591.
31. Smith AE, Slivicki RA, Hohmann AG, Crystal JD (2017): The chemotherapeutic agent paclitaxel selectively impairs learning while sparing source memory and spatial memory. Behav Brain Res 320:48–57.
32. Farra YM, Eden MJ, Coleman JR, Kulkarni P, Ferris CF, Oakes JM, *et al.* (2020): Acute neuroradiological, behavioral, and physiological effects of nose-only exposure to vaporized cannabis in C57BL/6 mice. Inhal Toxicol 32:200–217.
33. Brenner DS, Golden JP, Gereau RW IV (2012): A novel behavioral assay for measuring cold sensation in mice. PLoS One 7:e39765.
34. Menon RS, Thomas CG, Gati JS (1997): Investigation of BOLD contrast in fMRI using multi-shot EPI. NMR Biomed 10:179–182.
35. Hoogenraad FG, Pouwels PJ, Hofman MB, Rombouts SA, Lavini C, Leach MO, *et al.* (2000): High-resolution segmented EPI in a motor task fMRI study. Magn Reson Imaging 18:405–409.
36. Poser BA, Norris DG (2009): Investigating the benefits of multi-echo EPI for fMRI at 7 T. NeuroImage 45:1162–1172.
37. Swisher JD, Sexton JA, Gatenby JC, Gore JC, Tong F (2012): Multi-shot versus single-shot pulse sequences in very high field fMRI: A comparison using retinotopic mapping. PLoS One 7:e34626.
38. Kang D, Sung YW, Kang CK (2015): Fast imaging technique for fMRI: Consecutive multishot echo planar imaging accelerated with GRAPPA technique. BioMed Res Int 2015:394213.
39. Harris HM, Sufka KJ, Gul W, ElSohly MA (2016): Effects of delta-9-tetrahydrocannabinol and cannabidiol on cisplatin-induced neuropathy in mice. Planta Med 82:1169–1172.
40. Marshell R, Kearney-Ramos T, Brents LK, Hyatt WS, Tai S, Prather PL, *et al.* (2014): In vivo effects of synthetic cannabinoids JWH-018 and JWH-073 and phytocannabinoid Δ9-THC in mice: Inhalation versus intraperitoneal injection. Pharmacol Biochem Behav 124:40–47.
41. Nguyen JD, Aarde SM, Vandewater SA, Grant Y, Stouffer DG, Parsons LH, *et al.* (2016): Inhaled delivery of Δ^9-tetrahydrocannabinol (THC) to rats by e-cigarette vapor technology. Neuropharmacology 109:112–120.
42. Javadi-Paydar M, Nguyen JD, Kerr TM, Grant Y, Vandewater SA, Cole M, *et al.* (2018): Effects of Δ9-THC and cannabidiol vapor inhalation in male and female rats. Psychopharmacology 235:2541–2557.
43. Lichtman AH, Poklis JL, Poklis A, Wilson DM, Martin BR (2001): The pharmacological activity of inhalation exposure to marijuana smoke in mice. Drug Alcohol Depend 63:107–116.
44. Varvel SA, Bridgen DT, Tao Q, Thomas BF, Martin BR, Lichtman AH (2005): Δ9-Tetrahydrocannbinol accounts for the antinociceptive, hypothermic, and cataleptic effects of marijuana in mice. J Pharmacol Exp Ther 314:329–337.
45. Zimmer A, Zimmer AM, Hohmann AG, Herkenham M, Bonner TI (1999): Increased mortality, hypoactivity, and hypoalgesia in cannabinoid CB1 receptor knockout mice. Proc Natl Acad Sci U S A 96:5780–5785.
46. Rock EM, Limebeer CL, Parker LA (2018): Effect of cannabidiolic acid and Δ^9-tetrahydrocannabinol on carrageenan-induced hyperalgesia and edema in a rodent model of inflammatory pain. Psychopharmacology 235:3259–3271.
47. Craft RM, Kandasamy R, Davis SM (2013): Sex differences in anti-allodynic, anti-hyperalgesic and anti-edema effects of Δ^9-tetrahydrocannabinol in the rat. Pain 154:1709–1717.
48. Atwal N, Casey SL, Mitchell VA, Vaughan CW (2019): THC and gabapentin interactions in a mouse neuropathic pain model. Neuropharmacology 144:115–121.
49. Casey SL, Atwal N, Vaughan CW (2017): Cannabis constituent synergy in a mouse neuropathic pain model. Pain 158:2452–2460.
50. Cox ML, Haller VL, Welch SP (2007): The antinociceptive effect of Delta9-tetrahydrocannabinol in the arthritic rat involves the CB_2 cannabinoid receptor. Eur J Pharmacol 570:50–56.
51. Williams J, Haller VL, Stevens DL, Welch SP (2008): Decreased basal endogenous opioid levels in diabetic rodents: Effects on morphine and delta-9-tetrahydrocannabinoid-induced antinociception. Eur J Pharmacol 584:78–86.
52. Cox ML, Haller VL, Welch SP (2007): Synergy between delta9-tetrahydrocannabinol and morphine in the arthritic rat. Eur J Pharmacol 567:125–130.
53. Palazzo E, de Novellis V, Petrosino S, Marabese I, Vita D, Giordano C, *et al.* (2006): Neuropathic pain and the endocannabinoid system in the dorsal raphe: Pharmacological treatment and interactions with the serotonergic system. Eur J Neurosci 24:2011–2020.
54. Petrosino S, Palazzo E, de Novellis V, Bisogno T, Rossi F, Maione S, *et al.* (2007): Changes in spinal and supraspinal endocannabinoid levels in neuropathic rats. Neuropharmacology 52:415–422.
55. Mucke M, Phillips T, Radbruch L, Petzke F, Hauser W (2018): Cannabis-based medicines for chronic neuropathic pain in adults. Cochrane Database Syst Rev 3:CD012182.

56. Andreae MH, Carter GM, Shaparin N, Suslov K, Ellis RJ, Ware MA, *et al.* (2015): Inhaled cannabis for chronic neuropathic pain: A meta-analysis of individual patient data. J Pain 16:1221–1232.
57. Schimrigk S, Marziniak M, Neubauer C, Kugler EM, Werner G, Abramov-Sommariva D (2017): Dronabinol is a safe long-term treatment option for neuropathic pain patients. Eur Neurol 78:320–329.
58. Turri M, Teatini F, Donato F, Zanette G, Tugnoli V, Deotto L, *et al.* (2018): Pain modulation after oromucosal cannabinoid spray (SATIVEX®) in patients with multiple sclerosis: A study with quantitative sensory testing and laser-evoked potentials. Medicines 5:59.
59. Langford RM, Mares J, Novotna A, Vachova M, Novakova I, Notcutt W, *et al.* (2013): A double-blind, randomized, placebo-controlled, parallel-group study of THC/CBD oromucosal spray in combination with the existing treatment regimen, in the relief of central neuropathic pain in patients with multiple sclerosis. J Neurol 260:984–997.
60. Wade DT, Makela P, Robson P, House H, Bateman C (2004): Do cannabis-based medicinal extracts have general or specific effects on symptoms in multiple sclerosis? A double-blind, randomized, placebo-controlled study on 160 patients. Mult Scler 10:434–441.
61. Abrams DI, Jay CA, Shade SB, Vizoso H, Reda H, Press S, *et al.* (2007): Cannabis in painful HIV-associated sensory neuropathy: A randomized placebo-controlled trial. Neurology 68:515–521.
62. Ware MA, Martel MO, Jovey R, Lynch ME, Singer J (2018): A prospective observational study of problematic oral cannabinoid use. Psychopharmacology 235:409–417.
63. Weizman L, Dayan L, Brill S, Nahman-Averbuch H, Hendler T, Jacob G, *et al.* (2018): Cannabis analgesia in chronic neuropathic pain is associated with altered brain connectivity. Neurology 91:e1285–e1294.
64. Suzuki R, Rygh LJ, Dickenson AH (2004): Bad news from the brain: Descending 5-HT pathways that control spinal pain processing. Trends Pharmacol Sci 25:613–617.
65. Bannister K, Dickenson AH (2016): What do monoamines do in pain modulation? Current Opin Support Palliat Care 10:143–148.
66. Lin H, Heo BH, Kim WM, Kim YC, Yoon MH (2015): Antiallodynic effect of tianeptine via modulation of the 5-HT_7 receptor of GABAergic interneurons in the spinal cord of neuropathic rats. Neurosci Lett 598:91–95.
67. Avila-Rojas SH, Velazquez-Lagunas I, Salinas-Abarca AB, Barragan-Iglesias P, Pineda-Farias JB, Granados-Soto V (2015): Role of spinal 5-HT_{5A}, and 5-$HT_{1A/1B/1D}$, receptors in neuropathic pain induced by spinal nerve ligation in rats. Brain Res 1622:377–385.
68. Suzuki R, Morcuende S, Webber M, Hunt SP, Dickenson AH (2002): Superficial NK1-expressing neurons control spinal excitability through activation of descending pathways. Nat Neurosci 5:1319–1326.
69. Herkenham M, Lynn AB, Johnson MR, Melvin LS, de Costa BR, Rice KC (1991): Characterization and localization of cannabinoid receptors in rat brain: A quantitative in vitro autoradiographic study. J Neurosci 11:563–583.
70. Matsuda LA, Bonner TI, Lolait SJ (1993): Localization of cannabinoid receptor mRNA in rat brain. J Comp Neurol 327:535–550.
71. Nakazi M, Bauer U, Nickel T, Kathmann M, Schlicker E (2000): Inhibition of serotonin release in the mouse brain via presynaptic cannabinoid CB1 receptors. Naunyn Schmiedebergs Arch Pharmacol 361:19–24.
72. Egashira N, Mishima K, Iwasaki K, Fujiwara M (2002): Intracerebral microinjections of delta 9-tetrahydrocannabinol: Search for the impairment of spatial memory in the eight-arm radial maze in rats. Brain Res 952:239–245.
73. Moranta D, Esteban S, Garcia-Sevilla JA (2004): Differential effects of acute cannabinoid drug treatment, mediated by CB1 receptors, on the in vivo activity of tyrosine and tryptophan hydroxylase in the rat brain. Naunyn Schmiedebergs Arch Pharmacol 369:516–524.
74. Darmani NA, Janoyan JJ, Kumar N, Crim JL (2003): Behaviorally active doses of the CB1 receptor antagonist SR 141716A increase brain serotonin and dopamine levels and turnover. Pharmacol Biochem Behav 75:777–787.
75. Tzavara ET, Davis RJ, Perry KW, Li X, Salhoff C, Bymaster FP, *et al.* (2003): The CB1 receptor antagonist SR141716A selectively increases monoaminergic neurotransmission in the medial prefrontal cortex: Implications for therapeutic actions. Br J Pharmacol 138:544–553.
76. Britch SC, Goodman AG, Wiley JL, Pondelick AM, Craft RM (2020): Antinociceptive and immune effects of delta-9-tetrahydrocannabinol or cannabidiol in male versus female rats with persistent inflammatory pain. J Pharmacol Exp Ther 373:416–428.
77. Craft RM, Britch SC, Buzitis NW, Clowers BH (2019): Age-related differences in Δ^9-tetrahydrocannabinol-induced antinociception in female and male rats. Exp Clin Psychopharmacol 27:338–347.
78. Craft RM, Wakley AA, Tsutsui KT, Laggart JD (2012): Sex differences in cannabinoid 1 vs. cannabinoid 2 receptor-selective antagonism of antinociception produced by delta9-tetrahydrocannabinol and CP55, 940 in the rat. J Pharmacol Exp Ther 340:787–800.
79. Tseng AH, Harding JW, Craft RM (2004): Pharmacokinetic factors in sex differences in delta 9-tetrahydrocannabinol-induced behavioral effects in rats. Behav Brain Res 154:77–83.
80. Wakley AA, Wiley JL, Craft RM (2014): Sex differences in antinociceptive tolerance to delta-9-tetrahydrocannabinol in the rat. Drug Alcohol Depend 143:22–28.
81. Gorges M, Roselli F, Muller HP, Ludolph AC, Rasche V, Kassubek J (2017): Functional connectivity mapping in the animal model: Principles and applications of resting-state fMRI. Front Neurol 8:200.
82. Liang Z, King J, Zhang N (2012): Intrinsic organization of the anesthetized brain. J Neurosci 32:10183–10191.
83. Vincent JL, Patel GH, Fox MD, Snyder AZ, Baker JT, Van Essen DC, *et al.* (2007): Intrinsic functional architecture in the anaesthetized monkey brain. Nature 447:83–86.
84. Gozzi A, Schwarz AJ (2016): Large-scale functional connectivity networks in the rodent brain. NeuroImage 127:496–509.
85. Guilfoyle DN, Gerum SV, Sanchez JL, Balla A, Sershen H, Javitt DC, *et al.* (2013): Functional connectivity fMRI in mouse brain at 7T using isoflurane. J Neurosci Methods 214:144–148.
86. Jonckers E, Delgado y Palacios R, Shah D, Guglielmetti C, Verhoye M, Van der Linden A (2014): Different anesthesia regimes modulate the functional connectivity outcome in mice. Magn Reson Med 72:1103–1112.
87. Yang C, Zhang L, Hao H, Ran M, Li J, Dong H (2019): Serotonergic neurons in the dorsal raphe nucleus mediate the arousal-promoting effect of orexin during isoflurane anesthesia in male rats. Neuropeptides 75:25–33.